Elucidating the relations among seeded image segmentation methods and their possible extensions

Paulo A.V. Miranda
Department of Computer Science
IME – University of São Paulo (USP)
05508-090, São Paulo, SP, Brazil
Email: pavmbr@yahoo.com.br

Alexandre X. Falcão
Information Systems Department
LIV – Institute of Computing – Unicamp
CP 6176, 13084-971, Campinas, SP, Brazil
Email: afalcao@ic.unicamp.br

Abstract—Many image segmentation algorithms have been proposed, specially for the case of binary segmentation (object/background) in which hard constraints (seeds) are provided interactively. Recently, several theoretical efforts were made in an attempt to unify their presentation and clarify their relations. These relations are usually pointed out textually or depicted in the form of a table of parameters of a general energy formulation. In this work we introduce a more general diagram representation which captures the connections among the methods, by means of conventional relations from set theory. We formally instantiate several methods under this diagram, including graph cuts, power watersheds, fuzzy connectedness, grow cut, distance cuts, and others, which are usually presented as unrelated methods. The proposed diagram representation leads to a more elucidated view of the methods, being less restrictive than the tabular representation. It includes new relations among methods, besides bringing together the connections gathered from different works. It also points out some promising unexplored intermediate regions, which can lead to possible extensions of the existing methods. We also demonstrate one of such possible extensions, which is used to effectively combine the strengths of region and local contrast features.

Keywords-graph search algorithms; image foresting transform; graph-cut segmentation; watersheds; fuzzy connectedness;

I. Introduction

Image segmentation involving the extraction of an object from a background is a well pursued topic in image processing and computer vision. However, in order to guarantee reliable and accurate results, user supervision is still required in several segmentation tasks, such as the extraction of poorly defined structures in medical imaging and arbitrary objects in natural images. These problems motivated the development of several different methods for semi-automatic segmentation, aiming to minimize the user involvement and time required without compromising accuracy and precision.

These methods are usually divided in three classes, depending on the type of user input: 1) Initial contour/surface, 2) boundary-based constraints (anchor points), 3) region-based constraints (seeds).

On the first type, the user specifies an initial curve, close to the target boundary, which deforms automatically usually evolving into a local minimum that is returned as the final segmentation. This class includes the family of *active contour* (*snakes*) [1] and *level set* methods [2], [3].However, a problem associated with these methods is that when the returned result is not satisfactory, the user options are parameter adjustments or re-initialization (with a new input curve), which may be difficult for a non-expert user.

The second class, includes mainly *live wire* (*intelligent scissors*) [4], [5] and its extensions [6], [7], [8], and some snakes variants, which detect the global minimum of an active contour model's energy between two end points [9]. In relation to other methods from the first class, like *snakes* [1], live wire provides much tighter control to users since the desired path can be interactively selected from multiple candidate paths. More recently, the *riverbed* [10] approach was also proposed in order to handle complex shapes without shortcutting the boundary. However, one disadvantage of the methods under this class is that they are usually hard to be extended to multidimensional images [11].

The third class comprises seed-based image segmentation methods which adopt basically the following steps: The user provides a partial labelling of the image by placing hard constraints (known as seeds). After that, the seed's labels are propagated to all unlabeled regions by following some optimum criterion, such that a complete labeled image is constructed. Correction of wrongly segmented parts is accomplished by the addition and/or removal of seeds followed by the recomputation of the segmentation. This class encloses many of the most prominent methods for general purpose segmentation. In this work, we focus on this seed-based class, although some ideas presented here (e.g., the diagram representation) can be easily adapted to the other classes.

Several seed-based image segmentation methods have been developed based on different theories, supposedly not related, leading to different frameworks, such as watershed [12], [13], random walks [14], fuzzy connectedness [15], [16], graph cuts [17], [18], distance cut [19], and grow cut [20]. However, they usually make direct/indirect use of some image-graph concept, such as arc weight between pixels, which may be interpreted as similarity, speed function, affinity, cost, distance; depending on different frameworks used.In view of this, recent works have started to seek for theoretical relations among different frameworks as an important topic of research [21], [22], [23], [24], [25], [26], [27]. In these works, the relations are usually textually presented [22], [23], [24], or they use a

tabular representation, where each cell content reflects a distinct method resulting from different parameter configurations of a generic energy formulation [25], [26], [27]. However, the tabular representation based on an unique general energy formulation has some drawbacks:

- The extension to include new algorithms usually involves the addition of more parameters in the general energy formulation (e.g., a second parameter in [27] was necessary in order to extend the previous work [25]). This limits the inclusion of more methods, given that, the addition of a third parameter would lead to a three-dimensional table which is hard to visualize.
- Only a few special cases of some methods can be represented in this table. For example, in [26] what they call a watershed is, in fact, only a specific solution within a wider universe of existing definitions of watershed [28], that can not be represented on that table cell[1]. Also many methods closely related to watershed are not included, such as the fuzzy connectedness family [29].
- In order to fit in a particular table cell, some methods are presented without considering explicitly important regularization parameters, that could be used to establish new connections with other methods (e.g., shortest paths).
- Lastly, the general energy formulation used is very complex (e.g., it involves a continuous solution that is later discretized on a second step), while some methods can be more naturally described using a more intuitive and simpler energy formulation already designed for hard segmentations, as presented in [23], [24].

In view of these problems, in this work we introduce a more general representation in the form of a diagram, which captures the connections among methods by means of conventional relations of set theory. We formally instantiate several methods under this diagram, including graph cuts, power watersheds, fuzzy connectedness, grow cut, distance cuts, and others. New relations among methods are depicted, as well others gathered from different works, which are all brought together in a common representation. The proposed diagram representation presents the following advantages:

- It allows to properly represent the full universe of solutions of each method.
- It leads to a more elucidated view of the methods, explicitly treating all parameters of each method.
- It is less restrictive than the tabular representation, and can be arbitrarily extended.
- It also points out some promising unexplored intermediate regions, which can lead to possible extensions of the existing methods.

The diagram representation is introduced in Section II. In Section III, we give a short overview of several seed-based methods, already pointing out existing and new connections by taking advantage of a more uniform and formal presentation. Section IV instantiates the diagram and presents a summary of

all relations depicted for quick reference. Possible extensions are discussed in Section V, including the demonstration of the combination of two methods yielding to new solutions over an unexplored region. Our conclusions are stated in Section VI.

II. DIAGRAM REPRESENTATION

We are restricting our analysis to the case of binary segmentation for sake of simplicity, and also because some involved methods are hard to be extended to multiple objects (e.g., graph cut). But it is important to note that the diagram here presented can be trivially extended to the analysis of segmentation involving multiple objects.

Since all methods to be included in the diagram can be reformulated based on image graphs (although the original papers sometimes ommit this), we decided to explain the ideas already focusing on image graphs, as exposed next.

A multi-dimensional and multi-spectral image $\hat{I}$ is a pair $(\mathcal{I}, \vec{I})$ where $\mathcal{I} \subset Z^n$ is the image domain and $\vec{I}(p)$ assigns a set of m scalars $I_i(p)$, $i = 1, 2, \ldots, m$, to each pixel $p \in \mathcal{I}$. The subindex i is removed when $m = 1$. An image $\hat{I}$ can be interpreted as a graph $G = (\mathcal{N}, \mathcal{A})$ whose nodes in $\mathcal{N}$ are image pixels in $\mathcal{I}$, and arcs (p, q) are defined by an *adjacency relation* $\mathcal{A} \subset \mathcal{N} \times \mathcal{N}$. We use $q \in \mathcal{A}(p)$ and $(p, q) \in \mathcal{A}$ to indicate that q is adjacent to p. For each arc (p, q) we have an associated arc weight $w(p, q)$. Although some methods can be directly executed over directed graphs, we will assume undirected graphs in order to standardize the discussion, i.e., $\mathcal{A}$ is taken as an irreflexive and symmetric relation, and $w(p, q) = w(q, p)$. For example, one can take $\mathcal{A}$ to consist of all pairs of nodes (p, q) in the Cartesian product $\mathcal{N} \times \mathcal{N}$ such that $d(p, q) \leq \rho$ and $p \neq q$, where $d(p, q)$ denotes the Euclidean distance and ρ is a specified constant (e.g., 4-neighborhood, when $\rho = 1$).

Some methods may require an extended graph with additional nodes and arcs (e.g., graph cut) but since for most of the methods these additions are usually completely disregarded, we will postpone their explanation to a more specific section.

A binary seed-based segmentation can be defined by a labeled image $\hat{L} = (\mathcal{I}, L)$, which must satisfy two sets of hard constraints, $\mathcal{S}_o \subset \mathcal{I}$ and $\mathcal{S}_b \subset \mathcal{I}$ ($\mathcal{S}_o \cap \mathcal{S}_b = \emptyset$), containing seed pixels selected inside and outside the object, respectively (i.e., $L(p) = 1$ if $p \in \mathcal{S}_o$, $L(p) = 0$ if $p \in \mathcal{S}_b$, and $L(p) \in \{0, 1\}$ otherwise).

For any input image graph $G = (\mathcal{N}, \mathcal{A})$ and seed set $\mathcal{S} = \mathcal{S}_o \cup \mathcal{S}_b$, the possible results of a method X are defined by its list of parameters $P = \{P_1, P_2, \ldots, P_k\}$ and by its internal free choices made in the case of multiple valid solutions for the selected parameter values.

To depict the relations among the methods, we introduce a diagram representation where each method X is represented by a set $X(P)$ of its possible parameters values and internal variability depicted as a simple closed curve. When X presents a unique solution for any image graph and seed set, its closed curve collapses to a single dot in our representation. The relations among the methods are captured by the following rules:

[1]On the later paper [27], the authors changed the name of this cell from "watershed" to the more specific "power watershed q=1".

- Two methods are considered to overlap when for any image graph $G = (\mathcal{I}, \mathcal{A})$ and seeds they can produce the same result for some proper selection of their parameters and internal choices. In this case their diagrams present an intersection.
- Two methods are disjoint if there exists an image graph and seed set for which they cannot guarantee the same solution for any selection of their parameters (although they may eventually produce the same result for some simple images).
- A method X is a subset of another method Y if for any image graph and seed set, all of its predicted solutions are also valid solutions of Y for some suitable parameter selection on that graph.
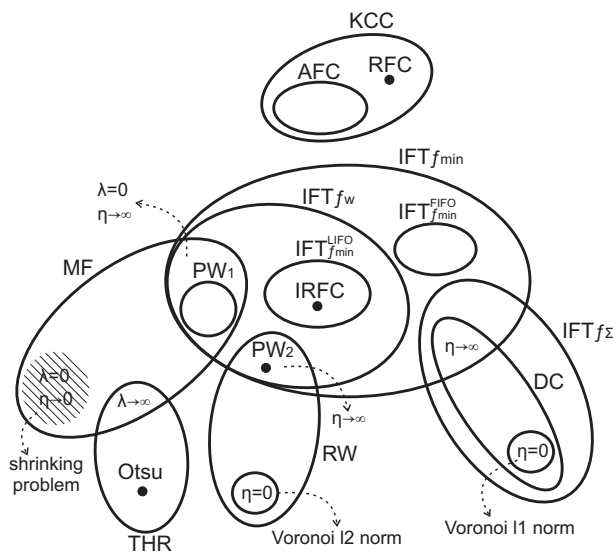

Fig. 1. Schematic representation of the relations between methods.

Figure 1 shows the proposed diagram for the seed-based methods, shown later in next section, as well their relations to be instantiated in details on Sections III and IV.

III. SEED-BASED SEGMENTATION METHODS

In order to instantiate the diagram, we give in this section a short description of several methods, including their list of considered parameters. But first, in Section III-A, we describe the *image foresting transform* (IFT) [21], which will be used as an underpinning in establishing the relations among several segmentation methods. In view to standardize the presentation, we adopted a canonical formulation of the arc weights $w(p, q)$ of the graph, so that:

1) For all $(p, q) \in \mathcal{A}$, we have that $0.0 < w(p, q) \leq 1.0$.
2) Low values are assigned to the arcs that cross the object's boundary, and high values to the remaining arcs (ideally ~ 0.0 and 1.0 respectively, although in practice this is usually not possible).

For example, we could use the complement of some normalized gradient magnitude on an arc as $w(p, q)$. When we refer

to a non-canonical weight, we will adopt a different symbol, such as $\delta(p, q)$.

Although several of the described approaches allow zero weighted arcs, we are avoiding such values in our discussion for the following reasons: In some frameworks, the connectivity through these weights is not allowed (i.e., zero-valued weights are interpreted as non-existing arcs). Moreover, zero-valued weights can also lead to additional differences between some approaches such as the creation of holes inside the objects. However, these differences are not that substantial, and they are usually implementation details that could be easily changed, so we decided to skip them in order to simplify our analysis. Also, zero-valued weights make impractical some transformations between dual representations of some methods due to division by zero.

A. Image Foresting Transform

The *image foresting transform* (IFT) [21] is a tool for the design of image processing operators based on *connectivity functions* (path-value functions) in graphs derived from the image. It has been used as an unifying framework for several image processing operators (not restricted to segmentation).

In the physical universe the IFT can be explained as a theory of the ordered formation of communities, in the mathematical universe as an image transformation into an optimum-path forest, and in the computational universe as an extension of Dijkstra's algorithm to more general connectivity functions and multiple sources [21].

Ordered formation of communities: Consider a population in which each individual has an intrinsic desire to lead groups. Individuals, with greater desire to become a leader, offer rewards to their acquaintances, inviting them to become part of their communities. If the offered reward is greater than their current desire, they consent to the proposal. A member of one of these communities, who was more rewarded, also invites his/her own friends, offering to them a reward to change to his/her community, and the process continues. However, a member never offers a reward higher than his/her own reward, and an individual only changes community when the new offered reward is greater than his/her current reward. The process follows the order of individuals with higher reward to the ones with lower reward through their acquaintances, until the population is divided into communities, such that each individual will belong to the group that offered the best (maximum) reward to him/her. At the end, a leader is an individual whose intrinsic desire is greater than any reward that was offered to him/her. A leader can also be a lonely individual who could not conquer anyone else.

From the mathematical point of view, each individual of the population corresponds to a node (pixel), his/her acquaintances are defined by the adjacency relation $\mathcal{A}$, and each community is given by an optimum-path tree. In the case of seed-based segmentation methods the leaders are always the seeds in $\mathcal{S}$

(roots by imposition) [2]. The seed sets $\mathcal{S}_o$ and $\mathcal{S}_b$ give us a partial labelling of the image, and this labelling is propagated to all pixels in $\mathcal{I}\backslash\mathcal{S}$, such that each community receives the same label of its leader.

The propagation of invitations from a leader to an individual q, follows a chain of friend pairs, forming a *path* $\pi = \langle p_1, p_2, \ldots, p_n \rangle$, $(p_i, p_{i+1}) \in \mathcal{A}$, $i = 1, 2, \ldots, n-1$, with origin at the leader $p_1 \in \mathcal{S}$, and terminus at $q = p_n \notin \mathcal{S}$. The reward offered to q through this path is defined by a *connectivity function* $f(\pi)$. Let π_q denote such a path with terminus at a node q. A path π_q is *optimum* if $f(\pi_q) \geq f(\tau_q)$ for any other path τ_q in $(\mathcal{N}, \mathcal{A})$, with terminus at q. The optimum-path value $V(q)$ is uniquely defined for all $q \in \mathcal{N}$ by $V(q) = \max_{\forall \pi_q \, in \, (\mathcal{N}, \mathcal{A})}\{f(\pi_q)\}$.

By assuming that the leaders are the seeds in $\mathcal{S}$, we can restrict the search for optimum paths only to paths starting in $\mathcal{S}$. So to simplify the discussion we will only define the connectivity functions for such paths (i.e., $p_1 \in \mathcal{S}$ and $p_i \notin \mathcal{S}$ for $i > 1$). Some commonly used functions are given below:

$$f_{max}(\pi) = \max_{i=1,2,\ldots,n-1} \delta_1(p_i, p_{i+1}) \qquad (1)$$

$$f_{min}(\pi) = \min_{i=1,2,\ldots,n-1} \delta_2(p_i, p_{i+1}) \qquad (2)$$

$$f_{\Sigma}(\pi) = \sum_{i=1,2,\ldots,n-1} \delta_3(p_i, p_{i+1}) \qquad (3)$$

$$f_{\Pi}(\pi) = \prod_{i=1,2,\ldots,n-1} \delta_4(p_i, p_{i+1}) \qquad (4)$$

The maximization of the reward offered by the connectivity functions always has a dual equivalent definition involving a minimization problem (i.e., $V(q) = \min_{\forall \pi_q \, in \, (\mathcal{N}, \mathcal{A})}\{f(\pi_q)\}$). For example, $V(q)$ must be maximized for $f_{min}(\pi)$, and $f_{max}(\pi)$ is used to solve the dual problem where $V(q)$ must be minimized while searching for optimum paths.

In the case of functions $f_{\Sigma}(\pi)$ and $f_{\Pi}(\pi)$, the dual definition is obtained by applying a transformation to the arc weights:

- Function $f_{\Sigma}(\pi)$: $V(q)$ must be minimized when $\delta_3 \geq 0.0$, and maximized for $\delta_3 \leq 0.0$. (i.e., the dual form is obtained by changing the sign of weights).
- Function $f_{\Pi}(\pi)$: $V(q)$ must be maximized when $0.0 < \delta_4 \leq 1.0$, and minimized for $\delta_4 \geq 1.0$ (i.e., the dual form is obtained by the inversion of weights δ_4^{-1}).

Moreover, functions $f_{\Sigma}(\pi)$ and $f_{\Pi}(\pi)$ are in fact equivalent for image segmentation, in the sense that they can be converted into each other by using a logarithmic transformation (one to one correspondence). Since the logarithm conserves the order of the connectivity values, it won't affect the final segmentation (Eq. 5).

$$\log(f_{\Pi}(\pi)) = \log\left(\prod_{i=1,2,\ldots,n-1} \delta_4(p_i, p_{i+1})\right)$$
$$= \sum_{i=1,2,\ldots,n-1} \log(\delta_4(p_i, p_{i+1})) \qquad (5)$$

---

[2]It is also possible to implement the IFT such that a seed may not become a leader, but since the seeds are selected by the user, it is usually preferable to assume them as hard constraints by using root imposition.

Therefore, in order to standardize the presentation, we consider only the functions that are indeed distinct, and we instantiate them in relation to the canonical weights $w(p, q)$, so that the optimum solution is obtained through a maximization, being consistent with the description given for the formation of communities:

$$f_{min}(\pi) = \min_{i=1,2,\ldots,n-1} w(p_i, p_{i+1}) \qquad (6)$$

$$f_{\Sigma}(\pi) = \sum_{i=1,2,\ldots,n-1} -[1.0 - w(p_i, p_{i+1})]^{\eta} \qquad (7)$$

where η is a regularization parameter that will be important for theoretical connections, and f_{Σ} uses a sum of negative terms in Eq. 7, because of the maximization problem, as explained earlier. Note that a division by any positive constant, to normalize the weights δ_2 and δ_3, does not affect the segmentation results of functions $f_{min}(\pi)$ and $f_{\Sigma}(\pi)$, therefore, we can always instantiate them based on the canonical weights without loss of generality.

From our discussion we have already two segmentation algorithms: $IFT_{f_{min}}(P = \emptyset)$ with no parameters and $IFT_{f_{\Sigma}}(P = \{\eta\})$ with one parameter. Both of these methods can present multiple valid solutions. The set $\mathcal{T}$ of all pixels with ambiguos labelling constitutes the tie-zone regions. These ambiguos pixels can be partitioned in several possible ways, and this is a free choice of these algorithms, being all connected solutions equally valid. We also include explicitly two commonly used subcases of $IFT_{f_{min}}$, denoted by $IFT_{f_{min}}^{FIFO}(P = \emptyset)$ and $IFT_{f_{min}}^{LIFO}(P = \emptyset)$, which are obtained by using the specific tie-breaking policies *FIFO* and *LIFO* [21], respectively.

B. Fuzzy connectedness: AFC, RFC, IRFC

In *absolute-fuzzy connectedness* (AFC) [30], the optimum-path values to all pixels in $\mathcal{I}\backslash\mathcal{S}_o$ are computed using only the seeds in $\mathcal{S}_o$, with function $f_{min}(\pi)$, such that the labelling of unmarked pixels is obtained by thresholding the resulting connectivity map $V_o(q)$:

$$V_o(q) = \max_{\forall \pi_q \, in \, (\mathcal{N}, \mathcal{A})|org(\pi_q)\in\mathcal{S}_o}\{f_{min}(\pi_q)\}, \qquad (8)$$

where $org(\pi_q)$ denotes the origin of the path π_q.

The resulting segmentation is defined as the maximal subset of $\mathcal{I}$, wherein all pixels q are reached by optimum paths whose values $V_o(q)$ are greater than or equal to a given threshold κ, or $q \in \mathcal{S}_o$ (i.e., we are assuming marker imposition).

In *relative-fuzzy connectedness* (RFC) [31], [15], a separate connectivity map $V_b(q)$ taking into account only the background seeds is also computed:

$$V_b(q) = \max_{\forall \pi_q \, in \, (\mathcal{N}, \mathcal{A})|org(\pi_q)\in\mathcal{S}_b}\{f_{min}(\pi_q)\}. \qquad (9)$$

The final segmentation is obtained by comparing the two connectivity maps $V_o(q)$ and $V_b(q)$, such that each pixel $q \in \mathcal{I}\backslash\mathcal{S}$ is given to the label with higher connectivity values. The tie regions of the RFC approach (i.e., $\mathcal{T}_{RFC} = \{q \in \mathcal{I}\backslash\mathcal{S} \mid V_o(q) = V_b(q)\}$), are larger than the tie zones produced by

the $IFT_{f_{min}}$ (i.e., $\mathcal{T}_{IFT_{f_{min}}} \subseteq \mathcal{T}_{RFC}$) [23]. In RFC, the tie-breaking policy is fixed such that $L(q) = 1$ only if $V_o(q) > V_b(q)$, and $L(q) = 0$ otherwise. Since the tie regions are not assigned to the object in RFC, the resulting object is always smaller or equal to the $IFT_{f_{min}}$ result, usually causing holes within the object.

Later, the *iterative relative-fuzzy connectedness* method (IRFC) [16] was proposed to improve RFC, aiming at the reduction of the tie regions $\mathcal{T}_{RFC}$. It is basically an iterative refinement strategy that imposes additional constraints based on results from the previous RFC iterations. In fact, $IFT_{f_{min}}$ already solves this problem due to the simultaneous label propagation from all seeds with online competition (i.e., $\mathcal{T}_{IRFC} = \mathcal{T}_{IFT_{f_{min}}}$). Indeed, IRFC was later reformulated based on $IFT_{f_{min}}$ [24], the only remaining difference is that the ties are left unassigned to the object on the IRFC approach, while $IFT_{f_{min}}$ also allows other tie-breaking policies.

From the above discussion, we have now other three algorithms: $RFC(P = \emptyset)$ and $IRFC(P = \emptyset)$ with no parameters, and $AFC(P = \{\kappa\})$ with one threshold parameter[3]. Both RFC and $IRFC$ produce unique segmentation results for any image graph, due to their conservative tie-breaking policy. Also, there is an AFC extension called κ-*connected components* (KCC) [32], which considers the resulting object as the union of all AFC results computed separately, with a different threshold κ_i for each seed in $\mathcal{S}_o$. The algorithm $KCC(P = \{\kappa_1, \kappa_2, \ldots, \kappa_{|\mathcal{S}_o|}\})$ has $|\mathcal{S}_o|$ parameters.

C. GrowCut

In *GrowCut* (GROW) [20], a new iterative algorithm for image segmentation is proposed based on Cellular Automata for solving pixel labelling. The segmentation is refined with each iteration according to an automata evolution rule. The calculation continues until the automaton converges to a stable configuration.

Accoring to the code in [20], during the local evolution rule, a pixel is attacked by all its neighbors, and it is conquered by a neighbor if the attack force is greater than its strength. This is closely related to the theory of ordered formation of communities presented earlier (see Section III-A), where the attack force corresponds to the reward offered, the defender's strength corresponds to the best reward he/she received so far (which is set initially as his/her intrinsic desire to lead groups), and "conquering" translates into "becoming part of a community". The only difference is that it is an unordered formation theory, leading to parallel implementations of the IFT [33]. Therefore, the results of the proposed GrowCut algorithm are in fact equivalent to the results obtained by IFT with connectivity function $f_\Pi(\pi)$ (the attack force is defined by a product), which are in turn equivalent to IFT with $f_\Sigma(\pi)$ as pointed earlier. But the implementation presented in [20] is slower for sequential processing, with resemblances to old fuzzy connectedness implementations based on unordered

---

[3]We assume that κ is selected such that the resulting object region does not invade the external seeds

propagation until convergence [31], [15], while the ordered propagation of IFT leads to linear time implementations, depending on the priority queue used [21], [6].

D. Distance cut

In *distance cut* (DC) [19], an algorithm based on additive connectivity functions $f_\Sigma(\pi)$ is presented. In fact this work also proposes solutions to the alpha matting problem, but we will focus only on the main core parts used for hard segmentation. Basically, it starts computing two connectivity maps $V_o^\Sigma(q)$ and $V_b^\Sigma(q)$ separately for object and background, similar to what was done for RFC, but this time using the function $f_\Sigma(\pi)$.

$$V_o^\Sigma(q) = \max_{\forall \pi_q \ in \ (\mathcal{N}, \mathcal{A}) | \mathrm{org}(\pi_q) \in \mathcal{S}_o} \{f_\Sigma(\pi_q)\}, \qquad (10)$$

$$V_b^\Sigma(q) = \max_{\forall \pi_q \ in \ (\mathcal{N}, \mathcal{A}) | \mathrm{org}(\pi_q) \in \mathcal{S}_b} \{f_\Sigma(\pi_q)\}, \qquad (11)$$

where $\mathrm{org}(\pi_q)$ denotes the origin of the path π_q.

After computing $V_o^\Sigma(q)$ and $V_b^\Sigma(q)$, the probability of a pixel $q \in \mathcal{I} \backslash \mathcal{S}$ to be assigned to the object is taken as:

$$P_{obj}(q) = \frac{(V_o^\Sigma(q))^{-1}}{(V_o^\Sigma(q))^{-1} + (V_b^\Sigma(q))^{-1}}. \qquad (12)$$

A hard segmentation may be obtained by thresholding $P_{obj}(q)$ at 0.5. However, from our previous discussion relating RFC and $IFT_{f_{min}}$, we know that the tie regions may increase when we compute the connectivity maps separately for object and background. To understand this, lets consider the following example:

Let π_q be the best path from $\mathcal{S}_o$ to a pixel q, and let τ_q the best path from $\mathcal{S}_b$ to q. When there is simultaneous label propagation from all seeds with competition, π_q blocks τ_q (making impractical the path τ_q and its future extensions) if $f(\pi_q) > f(\tau_q)$, and the opposite is also valid when $f(\tau_q) > f(\pi_q)$. But if there is no competition (i.e., the connectivity maps are computed separately for object and background), then τ_q may be extended even when $f(\pi_q) > f(\tau_q)$, possibly leading to augmented paths that are as good as the best extensions from π_q to the same nodes, thus increasing the tie zones.

But, fortunately, in the case of f_Σ this problem is not possible due to the additive nature of the function. That is, the deficiencies of a bad path are inherited by all of its extensions, and this extra cost can not be eliminated. Therefore, in the example given, the extensions of the path τ_q will never be as good as the extensions from π_q when $f_\Sigma(\pi_q) > f_\Sigma(\tau_q)$.

As conclusion, we have that the tie regions of DC (i.e., $\mathcal{T}_{DC} = \{q \in \mathcal{I} \backslash \mathcal{S} \mid P_{obj}(q) = 0.5\}$) and the tie regions of IFT_{f_Σ} are the same (i.e., $\mathcal{T}_{DC} = \mathcal{T}_{IFT_{f_\Sigma}}$). The only remaining difference is that in DC the tie regions may only be assigned to either object or background, due to the thresholding solution (i.e., the object may be taken as $P_{obj}(q) \geq 0.5$ or as $P_{obj}(q) > 0.5$), while in IFT_{f_Σ} other partitions may be valid depending on the order of propagation of the elements inside the tie zones.

E. Maximum Spanning Forest & Power watershed

The $IFT_{f_{min}}$ algorithm [34], [35] captures the essential features of the *watershed transform from markers* (WT) [36], although there is no unique and precise definition for a watershed transform in the literature [37]. Indeed, it was proven that the tie zones of the $IFT_{f_{min}}$ include all solutions predicted by many discrete definitions of WT [28].

Recent works consider the watershed solution WT as a partition resulting from a *maximum spanning forest* (MSF) [13], [38]. The segmentation results by $IFT_{f_{min}}$ include all possible MSF-WT solutions among many others not predicted by the MSF-WT [28]. In particular, the segmentations obtained by $IFT_{f_{min}}$ using *LIFO* tie-breaking policy [21], or with fixed label (1 or 0) to all tie zones, always correspond to a valid MSF-WT segmentation [23]. More generally, we may also consider the IFT with the following connectivity function for a path $\pi = \langle p_1, p_2, \ldots, p_n \rangle$:

$$f_w(\pi) = w(p_{n-1}, p_n) \qquad (13)$$

As discussed in [21], this connectivity function $f_w(\pi)$ is not *smooth* [21], and therefore, it may not lead to an optimum-path forest. However, the IFT will still return a spanning forest, and in this case using $f_w(\pi)$, it will also be a maximum spanning forest [32]. To understand this, please note that the IFT using $f_w(\pi)$ with a single seed becomes essentially the Prim's algorithm [39]. By construction, the extension to multiple seeds naturally results in a maximum spanning forest. Therefore, from the above discussion we have other algorithm $IFT_{f_w}(P = \emptyset)$ with no parameters, which is equivalent to MSF-WT. This algorithm may present multiple valid solutions. One example of such ties are the ambiguos plateaus on the frontier[4]

In order to solve ambiguous plateaus, a family of methods called *power watersheds* (PW) [26], [27] was later proposed. In these methods a q-cut optimization is performed on the plateaus (e.g., a random walker [14]). However, some theoretical aspects may only be ensured if the proposed algorithm is executed over a reconstructed graph G'[5]. Therefore, the authors apply first a geodesic reconstruction on the weights before employing the proposed power watershed algorithm.

This reconstruction essentially increases the number of ambiguous plateaus, since it converts all unmarked maxima and their domes into plateaus. Moreover, since the $IFT_{f_{min}}$ performs simultaneously reconstruction and segmentation [40], its tie-zone regions $\mathcal{T}_{IFT_{f_{min}}}$ correspond exactly to all ambiguous plateaus of the reconstructed graph G'. Hence, the power watershed PW corresponds basically to a particular $\mathcal{T}_{IFT_{f_{min}}}$ solution, where the tie zones are treated by applying other segmentation methods over it (e.g., random walks when $q = 2$ [26]).

This combination of a geodesic reconstruction, followed by the power watershed algorithm with $q = 2$ as presented in [27],

---

[4]A plateau is a subgraph of G consisting of a maximal set of nodes connected with edges having the same weight.

[5]The optimality of the power watershed according to a general energy formulation is achieved if seeds are the only maxima in the image graph [26].

will be denoted here as algorithm $PW_2(P = \emptyset)$ which has no parameters. This method produces unique segmentation results for any image graph.

F. Graph cut: min-cut/max-flow

Interactive segmentation using the *min-cut/max-flow* algorithm [17] uses extended image graphs, where two terminal nodes s and t (*source* and *sink*) represent object and background, respectively. The terminal nodes are directly connected to all pixels $p \in \mathcal{I}$ by arcs (s, p) and (p, t). A faster version of the min-cut/max-flow algorithm from source to sink [41] is then used to compute a minimum-cut boundary among all labeled images $\hat{L} = (\mathcal{I}, L)$, according to the following equation:

$$
\begin{aligned}
E(\hat{L}) \; = & \sum_{\forall (p,q) \in \mathcal{A}|\; L(p)=1, L(q)=0} [w(p,q)]^\eta \\
& + \sum_{\forall p \in \mathcal{I}|\; L(p)=1} \delta(p,t) + \sum_{\forall p \in \mathcal{I}|\; L(p)=0} \delta(s,p) \quad (14)
\end{aligned}
$$

The weights $\delta(p, t)$ and $\delta(s, p)$ assigned to all $p \in \mathcal{I}$ are defined as follows:
- If $p \in \mathcal{S}_o$, then we set $\delta(s, p) = \infty$ and $\delta(p, t) = 0$.
- If $p \in \mathcal{S}_b$, then we set $\delta(s, p) = 0$ and $\delta(p, t) = \infty$.
- If $p \in \mathcal{I} \backslash \mathcal{S}$, then these weights are defined by Equations 15 and 16.

$$\delta(s, p) = \lambda \cdot M_o(p) \qquad (15)$$
$$\delta(p, t) = \lambda \cdot M_b(p). \qquad (16)$$

Where $M_o(p)$ and $M_b(p)$ are membership maps for object and background, respectively, computed for all $p \in \mathcal{I}$ by supervised learning from user selected scribbles; and $\lambda \geq 0$ specifies the relative importance of the arcs with the virtual nodes versus the arcs between pixels. When λ becomes low, we may face a *shrinking bias* leading to solutions with small cuts. In order to avoid this bias, we must compensate it by using higher η values [23]. On the other hand, when λ becomes too high, the method degenerates into a trivial thresholding (i.e., $L(p) = 1$ if $\delta(s, p) > \delta(p, t)$ and $L(p) = 0$ otherwise, for all $p \in \mathcal{I}$). If we assume $M_o(p) + M_b(p) = 1.0$ for all $p \in \mathcal{I}$, as desired for a surrogate of the probability, then this solution for high λ assumes the form $L(p) = 1$ if $M_o(p) > 0.5$, and $L(p) = 0$ otherwise, for all $p \in \mathcal{I} \backslash \mathcal{S}$ (the pixels in $\mathcal{S}$ have fixed labels).

Therefore, we have the min-cut/max-flow approach $MF(P = \{\eta, \lambda\})$ with two parameters. Note that, the usage of canonical weights in the first sum of Equation 14, does not lead to a loss of generality, since the division/normalization by any positive constant (applied to all arcs) does not alter the order of the cut values. Hence, a representation with canonical values is always possible.

IV. DIAGRAM INSTANTIATION

Figure 1 shows the proposed diagram for the seed-based methods. Several depicted connections were extensively discussed along this paper. We also included some other simple

methods on the diagram, as for example, THR stands for thresholding the membership map $M_o(p)$, followed by manual seed painting, which is related to graph cut as pointed out in Section III-F. We also show that the $IFT_{f_\Sigma}(P = \{\eta\})$ includes the *Voronoi l1 norm* as a special case when $\eta = 0$ (assuming 4-neighborhood). Next we show a quick reference index, pointing to the related papers or sections that contain the proper remark concerning each relation between methods.

The connections between $IFT_{f_{min}}$ and $MF(P = \{\eta, \lambda\})$ are given in [23], the relations between MSF-WT (i.e., IFT_{f_w}) and $MF(P = \{\eta, \lambda\})$ are given in [22], and the relations between IFT_{f_w} and $IFT_{f_{min}}$ are given in [28]. Furthermore, the proof that $IFT_{f_{min}}$ has no intersection with $AFC(P = \{\kappa\})$ and RFC is given in [23]. GrowCut is equivalent to $IFT_{f_\Sigma}(P = \{\eta\})$ as discussed on Section III-C. The relation between $IRFC$ and $IFT_{f_{min}}$ was given in [24], [29]. In [42], [43], it was shown that the RFC segmentation can be viewed to some extent as an AFC segmentation wherein the required threshold is determined automatically. However, in general, it is not possible to derive RFC objects via AFC segmentation (e.g., when there are more than two objects involved in RFC, or S contains three or more singletons, the thresholds for each seed need not be equal) [42], [43]. Nevertheless, KCC [32] can provide these different thresholds, including RFC as a particular case. In [42], [43], it was also proven that $IRFC$ cannot be represented via $AFC(P = \{\kappa\})$. The relation between $IFT_{f_\Sigma}(P = \{\eta\})$ and $DC(P = \{\eta\})$ was shown on Section III-D. The relation between $IFT_{f_\Sigma}(P = \{\eta\})$ and $IFT_{f_{min}}$ was empirically suggested in [44]. The proof that $IFT_{f_\Sigma}(P = \{\eta\})$ has no intersection with MSF-WT (i.e., IFT_{f_w}) is given by the counterexample of Figure 2. The relation between $IFT_{f_{min}}$ and PW_2 was discussed on Section III-E. The relations between *random walks* ($RW(P = \{\eta\})$) [14] and PW_2, are assuming that the necessary optimality conditions for PW_2 were satisfied (i.e., seeds are the only maxima), as proved in [27], in order to simplify the analysis.
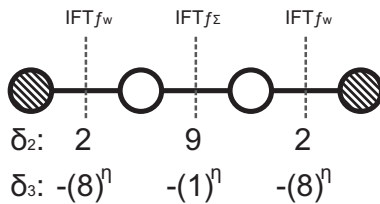
Fig. 2. A single 1D counterexample is sufficient to show that $IFT_{f_\Sigma}(P = \{\eta\})$ has no intersection with IFT_{f_w}. We use the weights δ_2 and δ_3 in Eqs. 2 and 3, as defined in Eqs. 6 and 7, but multiplied by a constant that does not affect the results (10 for δ_2, and 10^η for δ_3). The weights are indicated for all arcs, and the striped nodes are the seeds. According to $IFT_{f_{min}}$ any cut in this case is a valid solution, and all unmarked nodes form a tie zone. However, a valid MSF-WS solution must cut a weakest link interconnecting the seeds, so we have only the two possible solutions indicated (IFT_{f_w} using δ_2). While, only the central cut attends IFT_{f_Σ} for any η value.

V. POSSIBLE EXTENSIONS

From the diagram (Figure 1), it comes to our attention that there are some unexplored regions composed by intermediate
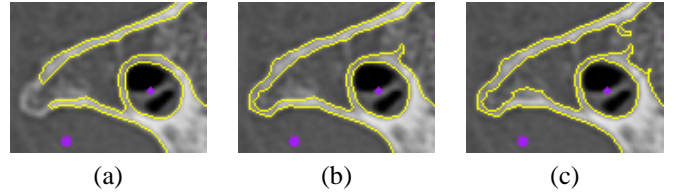

(a)   (b)   (c)

Fig. 3. Results of $IFT_{f_{min}}^\kappa$ for different α values (0, 0.1, 0.3) and fixed κ.

solutions between methods, such as AFC and $IFT_{f_{min}}$. Motivated by this observation, in this section we present an $IFT_{f_{min}}$ extension, denoted as $IFT_{f_{min}}^\kappa$, which combines AFC and the regular $IFT_{f_{min}}$. This extension provides more smooth and controllable transitions between the methods than in [32]. We will instantiate this combination, already focusing on a special case of practical interest.

If we execute AFC with $\delta(p, q) = \min(M_o(p), M_o(q))$, the method becomes a thresholding on the membership map M_o at level κ, followed by connectivity constraints. In other words, it returns all marked connected components of the thresholded image. This AFC solution subsumes *magic wand* from photoshop, being κ inversely related to the tolerance value. This AFC solution also does not suffer from the disconnection problem that affects the MF for high λ values.

Let's consider the following level based weight $\mu(p, q)$, which captures all κ threshold transitions over the map M_o.

$$\mu(p, q) = \begin{cases} 0 & \text{if } (M_o^{max}(p,q) \geq \kappa \text{ and} \\ & \quad M_o^{min}(p,q) < \kappa) \\ 1 & \text{otherwise} \end{cases}$$

where $M_o^{max}(p, q) = \max(M_o(p), M_o(q))$, and $M_o^{min}(p, q) = \min(M_o(p), M_o(q))$. Now consider a new graph $G' = (\mathcal{I}, \mathcal{A}')$, with modified weights $w'(p, q)$, such that $(p, q) \in \mathcal{A}'$, only if $w'(p, q) > 0$ and $(p, q) \in \mathcal{A}$.

$$w'(p, q) = \alpha \cdot \mu(p, q) + (1 - \alpha) \cdot w(p, q) \quad (17)$$

The $IFT_{f_{min}}^\kappa(P = \{\kappa, \alpha\})$ corresponds to a $IFT_{f_{min}}$ execution over the modified graph $G' = (\mathcal{I}, \mathcal{A}')$. Its result becomes the same as $AFC(P = \{\kappa\})$ when $\alpha = 1.0$[6], and it becomes a regular $IFT_{f_{min}}$ for $\alpha = 0.0$. For intermediate α values, it gives a mean unexplored behavior of the methods (Figure 3). From another point of view, we also have that the $\mu(p, q)$ component brings regional properties from the membership M_o into the method, helping the segmentation of thin parts, where the gradient (local contrast) does not solve well.

VI. CONCLUSION

The proposed diagram representation was instantiated with several state-of-the-art methods, giving a more elucidated view of their relations. Some of these relations were presented here for the first time, including the connections between GrowCut, IFT_{f_Σ}, and Distance Cut; IFT_{f_Σ} and $IFT_{f_{min}}$; RFC and KCC; PW_2 and IFT; among others. We also demonstrated an extended method, $IFT_{f_{min}}^\kappa(P = \{\kappa, \alpha\})$, which was

---

[6]Each seed $p \in \mathcal{S}_o$ must be selected inside regions such that $M_o(p) \geq \kappa$.

motivated by the unexplored regions of the diagram. As future work, we intend to extend these analyses to other classes of segmentation methods.

ACKNOWLEDGMENT

REFERENCES

[1] M. Kass, A. Witkin, and D. Terzopoulos, "Snakes: Active contour models," *Intl. Journal of Computer Vision*, vol. 1, pp. 321–331, 1987.

[2] J. Sethian, "Curvature and the evolution of fronts," *Comm. in Mathematical Physics*, vol. 101, pp. 487–499, 1985.

[3] ——, *Level Set Methods and Fast Marching Methods Evolving Interfaces in Computational Geometry, Fluid Mechanics, Computer Vision, and Materials Science*. Cambridge University Press, 1999.

[4] A. Falcão, J. Udupa, S. Samarasekera, S. Sharma, B. Hirsch, and R. Lotufo, "User-steered image segmentation paradigms: Live-wire and live-lane," *Graphical Models and Image Processing*, vol. 60, no. 4, pp. 233–260, Jul 1998.

[5] E. Mortensen and W. Barrett, "Interactive segmentation with intelligent scissors," *Graph. Models and Image Proc.*, vol. 60, pp. 349–384, 1998.

[6] A. Falcão, J. Udupa, and F. Miyazawa, "An ultra-fast user-steered image segmentation paradigm: Live-wire-on-the-fly," *IEEE Transactions on Medical Imaging*, vol. 19, no. 1, pp. 55–62, Jan 2000.

[7] H. Kang, "G-wire: A livewire segmentation algorithm based on a generalized graph formulation," *Pattern Recognition Letters*, vol. 26, no. 13, pp. 2042–2051, Oct 2005.

[8] F. Malmberg, E. Vidholm, and I. Nystrom, "A 3D live-wire segmentation method for volume images using haptic interaction," in *Discrete Geometry for Computer Imagery*, vol. 4245, 2006, pp. 663–673.

[9] L. Cohen and R.Kimmel, "Global minimum for active contour models: A minimal path approach," *Intl. Journal of Computer Vision*, vol. 24, no. 1, pp. 57–78, Aug 1997.

[10] P. Miranda, A. Falcão, and T. Spina, "The riverbed approach for user-steered image segmentation," in *Proc. of the International Conference on Image Processing (ICIP)*. Brussels, Belgium: IEEE, 2011, to appear.

[11] L. Grady, "Minimal surfaces extend shortest path segmentation methods to 3D," *IEEE Trans. Pattern Anal. Mach. Intell.*, vol. 32, no. 2, pp. 321–334, 2010.

[12] L. Vincent and P. Soille, "Watersheds in digital spaces: An efficient algorithm based on immersion simulations," *IEEE Transactions on Pattern Analysis and Machine Intelligence*, vol. 13, no. 6, Jun 1991.

[13] J. Cousty, G. Bertrand, L. Najman, and M. Couprie, "Watershed cuts: Thinnings, shortest path forests, and topological watersheds," *Trans. on Pattern Analysis and Machine Intelligence*, vol. 32, pp. 925–939, 2010.

[14] L. Grady, "Random walks for image segmentation," *IEEE Trans. Pattern Anaysis and Machine Intelligence*, vol. 28, no. 11, pp. 1768–1783, 2006.

[15] P. Saha and J. Udupa, "Relative fuzzy connectedness among multiple objects: Theory, algorithms, and applications in image segmentation," *Comp. Vision and Image Understanding*, vol. 82, no. 1, pp. 42–56, 2001.

[16] K. Ciesielski, J. Udupa, P. Saha, and Y. Zhuge, "Iterative relative fuzzy connectedness for multiple objects with multiple seeds," *Computer Vision and Image Understanding*, vol. 107, no. 3, pp. 160–182, 2007.

[17] Y. Boykov and M.-P. Jolly, "Interactive graph cuts for optimal boundary & region segmentation of objects in N-D images," in *International Conference on Computer Vision (ICCV)*, vol. 1, 2001, pp. 105–112.

[18] Y. Boykov and G. Funka-Lea, "Graph cuts and efficient N-D image segmentation," *Intl. Journal of Computer Vision*, vol. 70, no. 2, pp. 109–131, 2006.

[19] X. Bai and G. Sapiro, "Distance cut: Interactive segmentation and matting of images and videos," in *Proc. of the IEEE Intl. Conf. on Image Processing*, vol. 2, 2007, pp. II – 249–II – 252.

[20] V. Vezhnevets and V. Konouchine, ""growcut" - interactive multi-label N-D image segmentation by cellular automata," in *Proc. Graphicon.*, 2005, pp. 150–156.

[21] A. Falcão, J. Stolfi, and R. Lotufo, "The image foresting transform: Theory, algorithms, and applications," *IEEE Transactions on Pattern Analysis and Machine Intelligence*, vol. 26, no. 1, pp. 19–29, 2004.

[22] C. Allène, J. Audibert, M. Couprie, J. Cousty, and R. Keriven, "Some links between min-cuts, optimal spanning forests and watersheds," in *Proc. of the 8th Int. Symposium on Mathematical Morphology*, 2007, pp. 253–264.

[23] P. Miranda and A. Falcão, "Links between image segmentation based on optimum-path forest and minimum cut in graph," *Journal of Mathematical Imaging and Vision*, vol. 35, no. 2, pp. 128–142, 2009.

[24] K. Ciesielski, J. Udupa, A. Falcão, and P. Miranda, "Comparison of fuzzy connectedness and graph cut segmentation algorithms," in *Proc. of SPIE on Medical Imaging: Image Processing*, vol. 7962, 2011.

[25] A. Sinop and L.Grady, "A seeded image segmentation framework unifying graph cuts and random walker which yields a new algorithm," in *Proc. of the 11th International Conference on Computer Vision (ICCV)*. IEEE, 2007, pp. 1–8.

[26] C.Couprie, L.Grady, L.Najman, and H.Talbot, "Power watersheds: A new image segmentation framework extending graph cuts, random walker and optimal spanning forest," in *Proc. of the 12th International Conference on Computer Vision (ICCV)*. IEEE, 2009, pp. 731–738.

[27] ——, "Power watersheds: A unifying graph-based optimization framework," *Trans. on Pattern Anal. and Machine Intelligence*, vol. 99, 2010.

[28] R. Audigier and R. Lotufo, "Watershed by image foresting transform, tie-zone, and theoretical relationship with other watershed definitions," in *Proc. of the 8th Intl. Symposium on Mathematical Morphology and its Applications to Signal and Image Processing*, Oct 2007, pp. 277–288.

[29] ——, "Seed-relative segmentation robustness of watershed and fuzzy connectedness approaches," in *Proc. of the XX Brazilian Symposium on Computer Graphics and Image Processing*, Oct 2007, pp. 61–68.

[30] J. Udupa and S. Samarasekera, "Fuzzy connectedness and object definition: Theory, algorithms, and applications in image segmentation," *Graphical Models and Image Processing*, vol. 58, pp. 246–261, 1996.

[31] J. Udupa, P. Saha, and R. Lotufo, "Relative fuzzy connectedness and object definition: Theory, algorithms, and applications in image segmentation," *IEEE Transactions on Pattern Analysis and Machine Intelligence*, vol. 24, pp. 1485–1500, 2002.

[32] P. Miranda, A. Falcão, A. Rocha, and F. Bergo, "Object delineation by κ-connected components," *EURASIP Journal on Advances in Signal Processing*, pp. 1–14, 2008.

[33] F. Cappabianco, G. Araújo, and A. Falcão, "The image foresting transform architecture," in *IEEE Intl. Conf. on Field Programmable Technology (ICFPT)*, vol. 1, Dec 2007, pp. 137–144.

[34] R. Lotufo and A. Falcão, "The ordered queue and the optimality of the watershed approaches," in *Proceedings of the Intl. Symposium on Mathematical Morphology and its Applications to Signal and Image Processing (ISMM)*, vol. 18. Kluwer, Jun 2000, pp. 341–350.

[35] A. Falcão and F. Bergo, "Interactive volume segmentation with differential image foresting transforms," *IEEE Trans. on Medical Imaging*, vol. 23, no. 9, pp. 1100–1108, 2004.

[36] S. Beucher and F. Meyer, "The morphological approach to segmentation: The watershed transformation," in *Mathematical Morphology in Image Processing*. Marcel Dekker, 1993, ch. 12, pp. 433–481.

[37] J. Roerdink and A. Meijster, "The watershed transform: Definitions, algorithms and parallelization strategies," *Fundamenta Informaticae*, vol. 41, pp. 187–228, 2000.

[38] J. Cousty, G. Bertrand, L. Najman, and M. Couprie, "Watersheds, Minimum Spanning Forests, and the Drop of Water Principle," Université de Marne-la-Vallée, Tech. Rep. IGM2007-01, 2007.

[39] T. Cormen, C. Leiserson, and R. Rivest, *Introduction to Algorithms*. MIT, 1990.

[40] R. Lotufo, A. Falcão, and F. Zampirolli, "IFT-Watershed from gray-scale marker," in *Proceedings of the XV Brazilian Symposium on Computer Graphics and Image Processing*. IEEE, Oct 2002, pp. 146–152.

[41] Y. Boykov and V. Kolmogorov, "An experimental comparison of min-cut/max-flow algorithms for energy minimization in vision," *IEEE Transactions on Pattern Analysis and Machine Intelligence*, vol. 26, no. 9, pp. 1124–1137, Sep 2004.

[42] K. Ciesielski and J. Udupa, "Affinity functions in fuzzy connectedness based image segmentation i: Equivalence of affinities," *Computer Vision and Image Understanding*, vol. 114, no. 1, pp. 146–154, Jan 2010.

[43] ——, "Affinity functions in fuzzy connectedness based image segmentation ii: Defining and recognizing truly novel affinities," *Computer Vision and Image Understanding*, vol. 114, no. 1, pp. 155–166, Jan 2010.

[44] P. Miranda, A. Falcão, and J. Udupa, "Cloud bank: A multiple clouds model and its use in MR brain image segmentation," in *Proc. of the IEEE Intl. Symp. on Biomedical Imaging*, Boston, MA, 2009, pp. 506–509.